Fluid Effects on the Core Seismic Behavior of a Liquid Metal Reactor

Gyeong-Hoi Koo*, Jae-Han Lee
Korea Atomic Energy Research Institute,
P.O.Box 105, Yusong, Taejon 305-600, Korea

In this paper, a numerical application algorithm for applying the CFAM (Consistent Fluid Added Mass) matrix for a core seismic analysis is developed and applied to the 7-ducts core system to investigate the fluid effects on the dynamic characteristics and the seismic time history responses. To this end, three cases such as the in-air condition, the in-water condition without the fluid coupling terms, and the in-water condition with the fluid coupling terms are considered in this paper. From modal analysis, the core duct assemblies revealed strongly coupled out-of-phase vibration modes unlike the other cases with the fluid coupling terms considered. From the results of the seismic time history analysis, it was also verified that the fluid coupling terms in the CFAM matrix can significantly affect the impact responses and the seismic displacement responses of the ducts.

Key Words : Core Seismic Analysis, Fluid-Structure Interaction, Consistent Fluid Added Mass Matrix, FAMD (Fluid Added Mass and Damping) Code, Liquid Metal Reactor

1. Introduction

The LMR (Liquid Metal Reactor) cores are composed of several hundreds of duct sub-assemblies, which are in general hexagonal, such as the fuel elements, control rods, reflecting elements, neutron shield elements, and so on. These ducts have no intermediate supports and can be considered as self-standing hexagonal beams supported by a core support structure. These are submerged in liquid sodium with a very narrow gap space between the adjacent ones. Therefore, the core seismic behavior during an earthquake event may be subject to very complicated and highly non-linear characteristics due to the severe collision at the load pads and the dynamic fluid-structure interaction.

* Corresponding Author,
E-mail : ghkoo@kaeri.re.kr
TEL : +82-42-868-2950; **FAX** : +82-42-868-8363
Korea Atomic Energy Research Institute, P.O.Box 105, Yusong, Taejon 305-600, Korea. (Manuscript **Received** March 19, 2004; **Revised** August 31, 2004)

To secure the control rod insertion, the core structural integrity, and an accurate prediction of the reactivity insertion, the core seismic analysis should be carried out with a highly accurate method which can take into account the non-linear behavior, especially the fluid-structure interaction in a sodium condition. To verify the LMR core seismic technologies developed in different countries, the IAEA (International Atomic Energy Agency) Working Group on LMFBR (Liquid Metal Fast Breed Reactor) has approved the CRP (Coordinated Research Program) for an inter-comparison of the LMFR seismic analysis codes for the benchmark core mock-ups (Intercomparison of Liquid Metal Reactor Seismic Analysis Codes, 1993; 1994; 1995). In this study, most countries came up with different core seismic responses but noticed that the fluid-structure interaction effects is very important in the core seismic behavior analysis.

Actually, since the fluid-structure interaction analysis necessitates a highly nonlinear multi-field solution requiring a long computing time, it is not possible to directly consider the fluid-

structure interaction for the LMR core seismic time history analysis. Thus, a simple approach using the fluid added mass is often used in the seismic analysis (Koo and Lee, 2001).

In the case of the simple concentric cylinders submerged in a fluid, it is easy to calculate the 2×2 fluid added mass matrix by using the Fritz formula (Fritz, 1972). However, when the multi-bodies are immersed in a fluid, it is not easy to calculate the CFAM matrix. Then, it is necessary to perform the numerical calculations for each body's harmonic motion in the fluid. To do this, the FAMD code has been developed to calculate the CFAM matrix using the finite element method (Koo and Lee, 2003).

In this paper, an algorithm of the CFAM matrix, which can fully consider the fluid coupling terms in the matrix, for the core seismic analysis are developed and applied to a 7-ducts core system to investigate the fluid effects on the core seismic behavior such as the dynamic characteristics and the seismic time history responses. Three cases are investigated such as the in-air condition, the in-water condition without the fluid coupling terms, and the in-water condition with the fluid coupling terms.

2. Seismic Analysis Methods Considering the Fluid Effects

2.1 For a submerged concentric cylindrical system

When a single solid is submerged in the confined fluid field, the governing equation of the motion can be expressed as follows;

$$\begin{bmatrix} m_1 & 0 \\ 0 & m_2 \end{bmatrix}\begin{Bmatrix} \ddot{x}_1+\ddot{x}_g \\ \ddot{x}_2+\ddot{x}_g \end{Bmatrix}+\begin{bmatrix} k_1 & 0 \\ 0 & k_2 \end{bmatrix}\begin{Bmatrix} x_1 \\ x_2 \end{Bmatrix}+\begin{Bmatrix} F_{f1} \\ F_{f2} \end{Bmatrix}=\begin{Bmatrix} 0 \\ 0 \end{Bmatrix} \quad (1)$$

where m_1 and m_2 indicate the inertia masses, and k_1 and k_2 indicate the stiffnesses of the submerged solid and the outer container respectively. The third term in Eq. (1) represents the fluid reaction forces induced by a fluid-structure interaction during the seismic event. In general, these fluid forces can be simply expressed by the Fritz formula (Fritz, 1972), when the system consists of the concentric cylindrical structures with the fluid gap between the cylinders, as follows:

$$\begin{Bmatrix} F_{f1} \\ F_{f2} \end{Bmatrix}=\begin{bmatrix} \alpha M_1 & -(1+\alpha)M_1 \\ -(1+\alpha)M_1 & (1+\alpha)M_1+M_2 \end{bmatrix}\begin{Bmatrix} \ddot{x}_1+\ddot{x}_g \\ \ddot{x}_2+\ddot{x}_g \end{Bmatrix} \quad (2)$$

where $M_1=\rho_f\pi R_1^2 L$, $M_2=\rho_f\pi R_2^2 L$, $\alpha=(R_2^2+R_1^2)/(R_2^2-R_1^2)$, and $\ddot{x}_g$ is the seismic input acceleration. The terms of M_1 and M_2 indicate the mass of fluid with the meanings as follow;

M_1=mass of fluid displaced by the inner cylinder

M_2=mass of fluid that could fill the outer cylindrical cavity in the absence of the inner cylinder

Especially, M_1 has a meaning of the buoyant force of the inner cylinder. The symbol α has a meaning of the geometric factor relating with gap size.

After substituting Eq. (2) into Eq. (1), we can obtain the equation of the seismic motion as follows;

$$\begin{bmatrix} m_1+\alpha M_1 & -(1+\alpha)M_1 \\ -(1+\alpha)M_1 & m_2+(1+\alpha)M_1+M_2 \end{bmatrix}\begin{Bmatrix} \ddot{x}_1 \\ \ddot{x}_2 \end{Bmatrix} +\begin{bmatrix} k_1 & 0 \\ 0 & k_2 \end{bmatrix}\begin{Bmatrix} x_1 \\ x_e \end{Bmatrix}=-\ddot{x}_g\begin{Bmatrix} m_1-M_1 \\ m_2+M_2 \end{Bmatrix} \quad (3)$$

From the above equation, the off-diagonal terms in the inertia mass matrix cause the submerged inner cylinder to be dynamically coupled to the outer cylinder. These fluid coupled inertia terms have a negative sign and invoke an out-of-phase vibration between the two cylinders (Koo and Lee, 2001).

2.2 For a submerged multi-bodies system

Different from the simple concentric cylindrical system, when there are several solid bodies submerged in a confined fluid field, it might be difficult to treat the fluid-structure interaction problem between the solid bodies. In this paper, the simple fluid added mass approach is introduced to take into account the fluid effects in the seismic response analysis using the calculated CFAM matrix by the FAMD code (Koo and Lee, 2003).

The fluid-structure interaction behavior between the solid bodies submerged in the confined fluid as shown in Fig. 1 can be depicted by the fluid reaction forces, which can be determined for a unit amplitude oscillation of one body in each of the two orthogonal directions and no oscillations of the remaining fluid boundaries contacting with the other bodies. Each body has hydrodynamic reactions caused by an oscillation of itself, other bodies, and the outer container. In the FAMD code, the fluid added mass and damping of the solid bodies being represented by the consistent matrix form with the complex coupling terms can be obtained from the results of the 2-dimensional fluid-structure interaction analysis. Therefore, the fluid-structure interaction effects can be modeled by using the CFAM matrix in the core seismic analysis.

In using the CFAM matrix in modeling the submerged multi-bodies like a complex LMR core configuration, it is necessary to simplify the seismic analysis model with the conventional technology as a stick model using the lumped mass and damping system. Actually, the LMR core system has a complex 3-dimensional configuration as in Fig. 2, however a single- row stick model using only center row is generally used in the core seismic analysis as shown in Fig. 3. In this modeling method, each duct has simple beam properties and concentrated added masses and the gaps between ducts are modeled with gap springs and dampers.

To develop the application algorithm of the CFAM matrix in the LMR core seismic model, a general single row core modeling technology (Intercomparison of Liquid Metal Reactor Seismic Analysis Codes, 1993) as shown in Fig. 4 is used in this paper. In the figure, n is the number of ducts and m is the number of the nodes per duct. To apply the CFAM matrix to the analysis model, the coupling nodes are required in the model and it is necessary that the coupling nodes are located at the same coordinates in the vertical direction because the CFAM matrix is for the unit axial length obtained from the 2-dimensional fluid field.

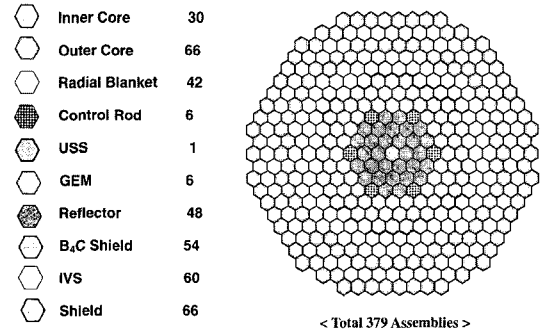

Fig. 2 Typical LMR core configurations

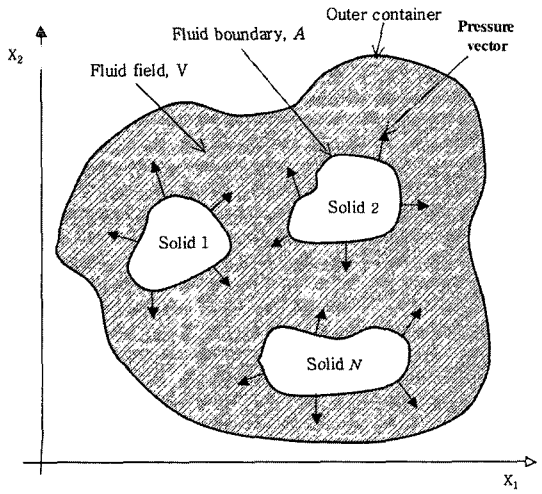

Fig. 1 Two-dimensional fluid field with the cross sections of N solid bodies

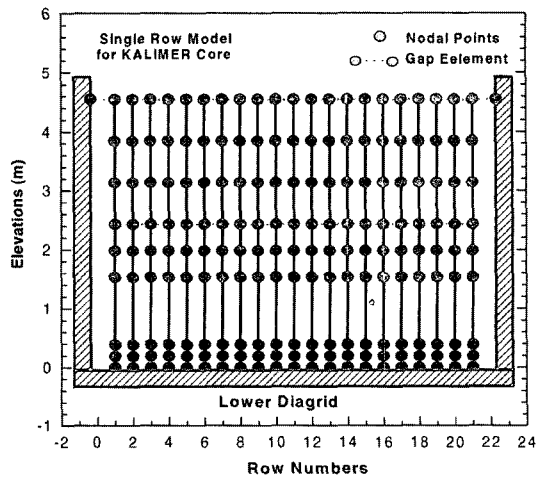

Fig. 3 Typical single-row core seismic analysis model

As shown in Fig. 4, when we define each set of the coupling nodes as a grid, the CFAM matrix is defined for each grid and the CFAM matrix can be expressed for the ith grid as follows ;

$$[\mathbf{CFAM}]_i = L_i \times \begin{bmatrix} M_{1,i}^{1,i} & M_{2,i}^{1,i} & M_{3,i}^{1,i} & \cdots & M_{n,i}^{1,i} \\ M_{1,i}^{2,i} & M_{2,i}^{2,i} & M_{3,i}^{2,i} & \cdots & M_{n,i}^{2,i} \\ M_{1,i}^{3,i} & M_{2,i}^{3,i} & M_{3,i}^{3,i} & \cdots & M_{n,i}^{3,i} \\ \vdots & \vdots & \vdots & \vdots & \vdots \\ M_{1,i}^{n,i} & M_{2,i}^{n,i} & M_{3,i}^{n,i} & \cdots & M_{n,i}^{n,i} \end{bmatrix}_i \quad (4)$$

$$i = 1, 2, 3, \cdots, m$$

where L_i is the applied length of the ith grid.

The applied length L_i will be given with the neighboring element lengths in Fig. 4 as follows ;

$$L_i = (Z_{i-1} + Z_i)/2, \quad i = 1, 2, 3, \cdots, m \quad (5)$$

In the above equation, Z_o and Z_m are zero.

For an example, the 7-ducts core system as shown in Fig. 5 can be modeled using a single central row with 5-sticks including the outer container. In this case, the CFAM matrix using in the core seismic analysis becomes a 5×5 matrix as follows ;

$$\begin{bmatrix} M_{1,i}^{1,i} & M_{2,i}^{1,i} & M_{3,i}^{1,i} & M_{4,i}^{1,i} & M_{5,i}^{1,i} \\ M_{1,i}^{2,i} & M_{2,i}^{2,i} & M_{3,i}^{2,i} & M_{4,i}^{2,i} & M_{5,i}^{2,i} \\ M_{1,i}^{3,i} & M_{2,i}^{3,i} & M_{3,i}^{3,i} & M_{4,i}^{3,i} & M_{5,i}^{3,i} \\ M_{1,i}^{4,i} & M_{2,i}^{4,i} & M_{3,i}^{4,i} & M_{4,i}^{4,i} & M_{5,i}^{4,i} \\ M_{1,i}^{5,i} & M_{2,i}^{5,i} & M_{3,i}^{5,i} & M_{5,i}^{5,i} & M_{5,i}^{5,i} \end{bmatrix}_i \quad (6)$$

Actually, the fluid gaps between the duct assembles in the LMR core are designed to be uniform, therefore the same fluid added mass matrix obtained by the FAMD code can be used for all the grids. However, when the fluid gaps are different in each sectional area along the fluid depth, the variable CFAM matrix by the FAMD code should be prepared and applied for each section separately.

The governing equation of a seismic motion including the fluid effects can be expressed with a simple lumped mass, damping, stiffness matrix, and the fluid reaction force as follows ;

$$[M]\{\ddot{x}_r + \ddot{x}_g\} + [C]\{\dot{x}_r\} + [K]\{x_r\} + \{F_f\} = 0 \quad (7)$$

where $\{x_r\}$ is the relative displacement for the input motion and $\ddot{x}_g$ is the seismic input ac -eleration.

The fluid reaction force term in Eq. (7) can be represented by using the CFAM matrix of Eq. (4) as follows ;

$$[F_f] = [\mathbf{CFAM}]\{\ddot{x}_r + \ddot{x}_g\} = [M_f]\{\ddot{x}_r + \ddot{x}_g\} \quad (8)$$

After substituting Eq. (8) into Eq. (7) and arranging the equation, Eq. (7) can be rewritten as follows ;

$$[M + M_f]\{\ddot{x}_r\} + [C]\{\dot{x}_r\} + [K]\{x_r\} = -[M + M_f]\{\ddot{x}_g\} \quad (9)$$

In the above equation, the obtained CFAM matrix, $[M_f]$ of each grid can be globally assembled step by step with the system mass matrix, $[M]$ for a core seismic analysis.

To solve Eq. (9), this paper introduces the

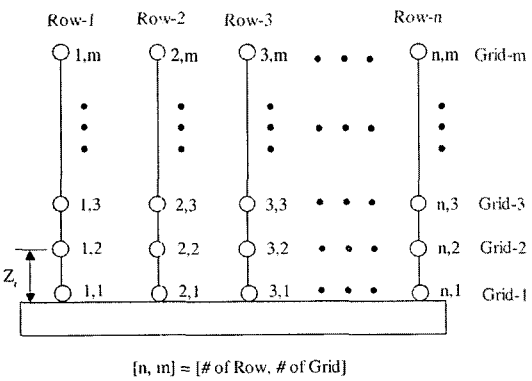

Fig. 4 Single-row core seismic analysis model with the CFAM matrix

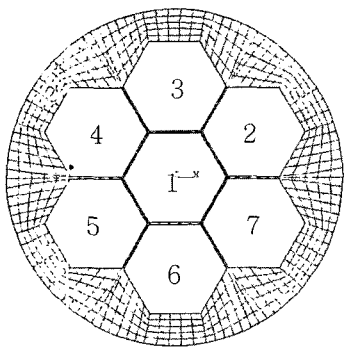

Fig. 5 Analysis model of the CFAM matrix for the 7-ducts system

Runge-Kutta numerical algorithm using the transformation vectors as follows;

$$y=\begin{Bmatrix} x_r \\ \dot{x}_r \end{Bmatrix},\ \dot{y}=\begin{Bmatrix} \dot{x}_r \\ \ddot{x}_r \end{Bmatrix} \tag{10, 11}$$

From Eq. (9) the $\{\ddot{x}_r\}$ can be expressed as follows;

$$\{\ddot{x}_r\}=-[M+M_f]^{-1}([C]\{\dot{x}_r\}+[K]\{x_r\} +[M+M_f]\{\ddot{x}_g\}) \tag{12}$$

After substituting Eq. (12) into Eq. (11), the $[n\times n]$ second order differential equation of Eq. (9) is transformed to the $[2n\times 2n]$ first order differential equation as follows;

$$\{\dot{y}\}=\begin{bmatrix} 0 & I \\ -[M+M_f]^{-1}[K] & -[M+M_f]^{-1}[C] \end{bmatrix}\{y\}+\begin{Bmatrix} 0 \\ -\{\ddot{x}_g\} \end{Bmatrix} \tag{13}$$

In general, it is known that the Runge-Kutta method gives more exact solution results when compared with the other direct integration algorithms. However, when the system matrix in the governing equation contains much higher natural frequency characteristics, this method has a severe disadvantage of the computing time. To resolve this problem, it is required to eliminate the unnecessary degree of freedom in the system matrix by the matrix condensation technique.

At first, to condensate the stiffness matrix, the matrix may be partitioned into the slave (eliminated) and master (no-eliminated) degree of freedoms as follows;

$$\begin{bmatrix} K_{aa} & K_{ac} \\ K_{ca} & K_{cc} \end{bmatrix}\begin{Bmatrix} U_a \\ U_c \end{Bmatrix}=\begin{Bmatrix} R_a \\ R_c \end{Bmatrix} \tag{14}$$

where U and R are the displacement and the load state vectors respectively, and the subscript a and c indicate the master and slave degree of freedom respectively. From Eq. (14), the slave state vectors may be written as follows;

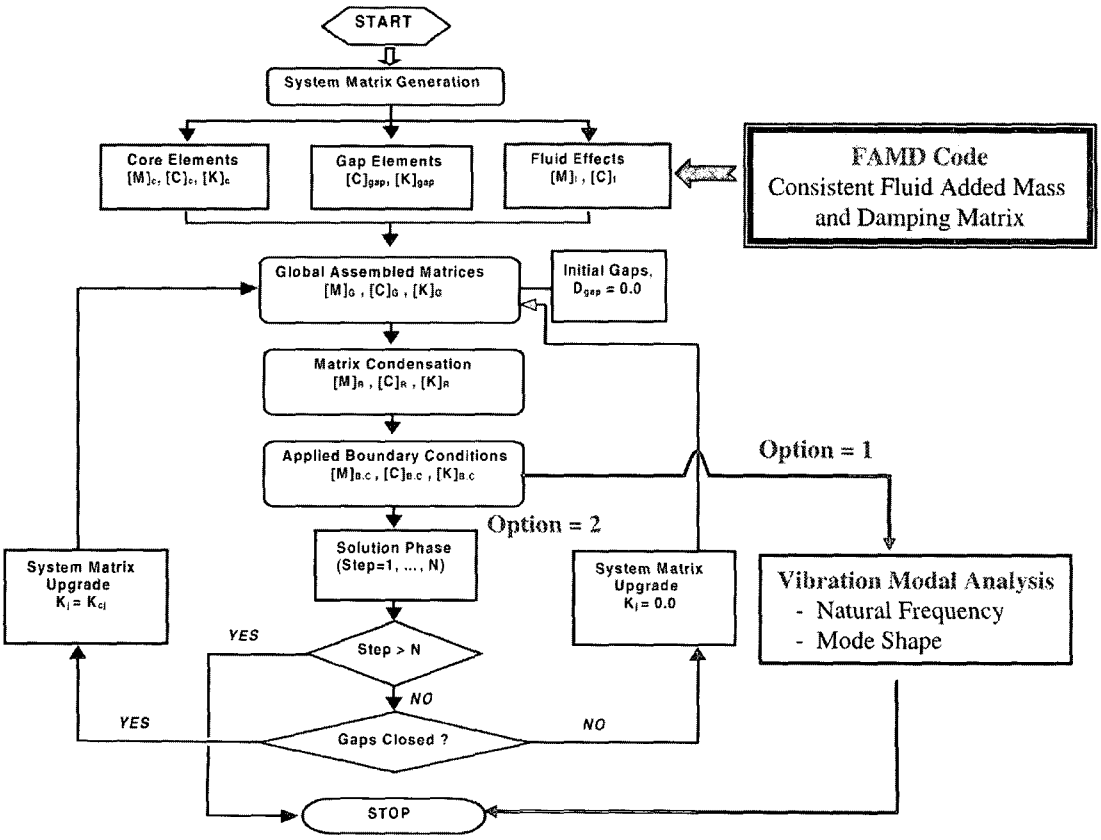

Fig. 6 General analysis procedure for the core seismic analysis

$$U_c = K_{cc}^{-1}(R_c - K_{ca}U_a) \quad (15)$$

After substituting Eq. (15) into Eq. (14), the equation with the condensed stiffness matrix can be obtained as follows;

$$(K_{aa} - K_{ac}K_{cc}^{-1}K_{ca})\,U_a = R_a - K_{ac}K_{cc}^{-1}R_c \quad (16)$$

For the mass condensation, using the energy balance method the condensed mass matrix may be expressed as follows (Cook et al., 1989);

$$M_{con} = M_{aa} + K_{ca}^{T}K_{cc}^{-1}M_{cc}K_{cc}^{-1}K_{ca} - K_{ca}^{T}K_{cc}^{-1}M_{ca} - M_{ac}K_{cc}^{-1}K_{ca} \quad (17)$$

Figure 6 shows the general flow diagram of the core seismic analysis used in this paper.

3. Examples of Application

As an example of the application to investigate the fluid effects on the core seismic behavior in a LMR, the 7-ducts system submerged in a confined fluid field is considered in this paper as shown in Fig. 7. The main body of the ducts has a uniform hexagonal section and the lower parts of the ducts are modeled as a nosepiece with cylindrical sections, which is fixed at the lower plate. The full length of the duct is 100 cm including the 10 cm nosepiece. The length of the flat-to-flat is 4 cm and the thickness of a duct cylinder is 0.2 cm. The gap distance between ducts is 0.2 cm and the diameter of an outer cylinder is 16.2 cm.

The 7-ducts system used in the analysis consists of two types of ducts. A center duct has a 1.0 cm outer diameter of a nosepiece and the 6 outer ducts have a 1.4 cm outer diameter which gives a stronger stiffness than the center duct.

3.1 Calculation of the CFAM matrix

To obtain the CFAM matrix, the analysis of the fluid reaction force for the 7-ducts system was carried out using the FAMD code. Figure 8 shows the finite element analysis model used in this paper. The nodal coordinates and the finite elements in the model are generated using the ANSYS preprocessor. The total number of nodes and elements for a fluid field are 1054 and 288 respectively.

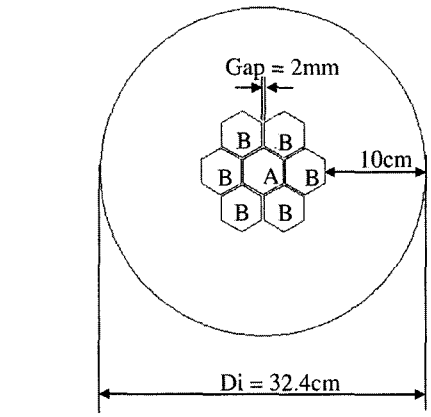

(a) Top view

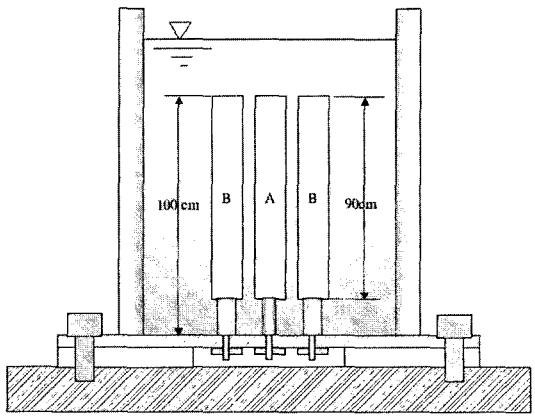

(b) Side view for the single row

Fig. 7 Dimensions of the 7-ducts system used in the analysis

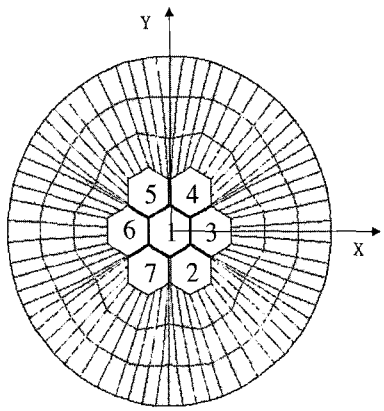

Fig. 8 Finite analysis model for the calculation of the CFAM Matrix

Table 1 The calculated CFAM matrix for the 7-ducts system (kg)

	1-X	2-X	3-X	4-X	5-X	6-X	7-X	8-X
1-X	10.55					Symmetry		
2-X	0.37	4.72						
3-X	−4.75	1.18	7.06					
4-X	0.37	0.43	1.14	4.72				
5-X	0.37	−0.07	−1.10	−3.10	4.72			
6-X	−4.75	−1.11	−1.15	−1.11	1.18	7.06		
7-X	0.37	−3.10	−1.10	−0.07	0.43	1.14	4.72	
8-X	−4.1	−4.18	−2.88	−4.18	−4.18	−2.88	−4.18	108.10

Table 1 shows the calculated fluid added mass matrix. As shown in the table, the central duct, duct-1 has a maximum fluid added mass, $M_1^1=$ 10.55 kg due to the effect of the small fluid gaps surrounding it. For duct-6 and duct-3 parallel to the duct-1, the fluid added masses are $M_3^3=M_6^6=7.06$ kg, which are less than the central duct-1. The coupling fluid added masses between duct-1 and the outer ducts are $M_3^1=M_6^1=-4.75$ kg. These coupling terms are almost half of anddud are expected to significantly affect the dynamic behavior of M_1^1 the given system.

3.2 Core seismic analysis model

Figure 9 shows the single row analysis model with 5-sticks for the 7-ducts core system used in this paper. This model consists of 35 nodes, 18 beam elements, 4 gap elements, and 6 grids for applying the CFAM matrix.

For the impact behavior between the closely spaced ducts, it is assumed that the impacts only occur at the top end location of the ducts and this can be modeled with the gap elements consisting of the impact spring and damp as shown in Fig. 9. The gap sizes are 2 mm between the ducts and 100 mm between the outer duct (Row-L and Row-R) and the outer container.

Because the input values of an impact stiffness and damping between the ducts may significantly affect the core seismic behavior during a seismic event, these have to be determined cautiously by experiments or analysis. In this paper, the numerical analysis method by the conventional unit

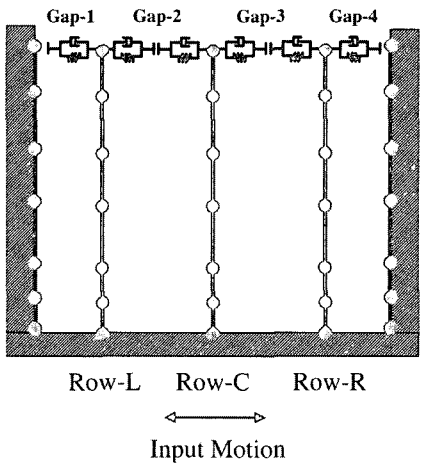

Fig. 9 Core seismic analysis model for the 7-ducts system

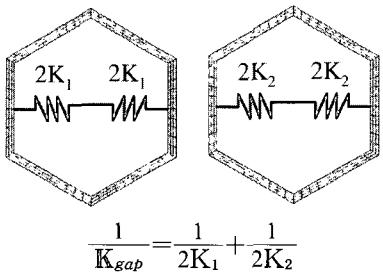

Fig. 10 Concept of impact stiffness calculation between the adjacent ducts

stiffness analysis is used for determining the impact stiffness. As shown in Fig. 10, the impact stiffness, $\mathbb{K}_{gap}$ between the neighboring ducts can be simply determined using both the stiffness values of the ducts by the following equation.

$$\frac{1}{\mathbb{K}_{gap}}=\frac{1}{2\mathbb{K}_1}+\frac{1}{2\mathbb{K}_2} \tag{18}$$

From the determined impact stiffness for the gap, the impact damping, $\mathbb{C}_{gap}$ can be determined using the following relationship (Intercomparison of Liquid Metal Reactor Seismic Analysis Codes, 1995).

$$\mathbb{C}_{gap}=\mathbb{K}_{gap}\frac{(1-e^2)\,t}{\pi} \tag{19}$$

where t is the impact duration and e is the contact coefficient of the restitution. In general, e is 0.55 for a steel-steel contact.

Table 2 Results of the calculated natural frequencies

	Row-L			Row-C			Row-R		
	Air	Water (Diagonal)	Water (CFAM)	Air	Water (Diagonal)	Water (CFAM)	Air	Water (Diagonal)	Water (CFAM)
1st	12.3	6.7	6.3	6.4	3.0	2.9	12.3	6.7	6.3
2nd	186.5	96.4	9.3	164.1	71.2	9.3	186.5	96.4	9.3
3rd	550.3	247.5	64.0	423.9	157.3	64.0	550.3	247.5	64.0

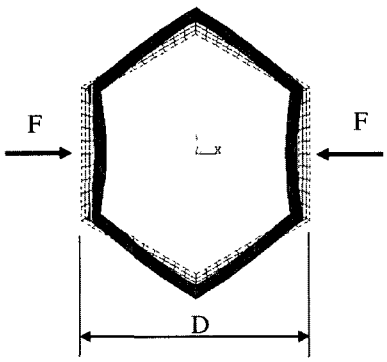

Fig. 11 Finite element analysis calculating the duct stiffness

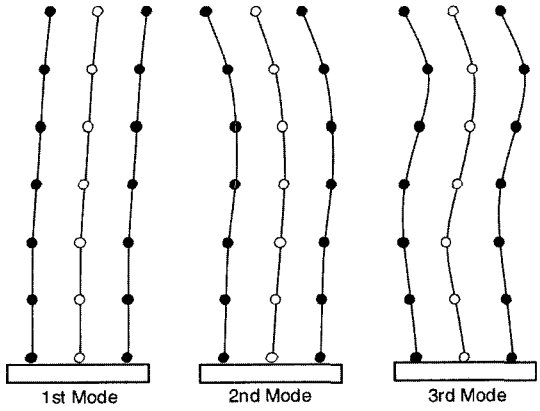

Fig. 12 Vibration mode shapes in the case of no fluid coupling terms

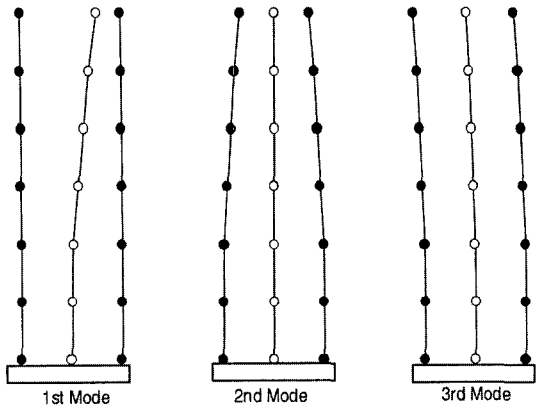

Fig. 13 Vibration mode shapes in the case of fluid coupling terms

The stiffness values for each duct can be determined from the unit stiffness analysis using the finite element analysis as shown in Fig. 11. The stiffness value of the duct will be simply calculated from the following equation ;

$$\mathbf{K}_{el}=\frac{\mathbf{F}}{\Delta \mathbf{D}} \tag{20}$$

The impact stiffness and damping values obtained by the numerical analysis in this paper are as follows ;

$$\mathbf{K}_{gap}=\mathbf{K}_{el}=\frac{\mathbf{F}}{\Delta \mathbf{D}}=\frac{1000}{8.2062E-6}=121.8\ \mathrm{MN/m}$$

$$\mathbf{C}_{gap}=\mathbf{K}_{gap}\frac{(1-e^2)\,t}{\pi}=121.8E6\frac{(1-0.55^2)\,0.1}{\pi}$$
$$=2.7\ \mathrm{MNs/m}$$

3.3 Vibration modal characteristics

For a given analysis model, the vibration modal analyses are carried out to investigate the fluid effects on the dynamic characteristics. To do this, three conditions are considered 1) in-air condition, 2) in-water condition without the fluid coupling mass terms, and 3) in-water condition with the fluid coupling mass terms.

Table 2 shows the results of the comparison of the natural frequencies for each condition. For the in-air condition, the 1st natural frequency is 12.3 Hz for Row-L and Row-R, 6.4 Hz for Row-C independently. For the in-water condi-

tion without the fluid coupling mass terms, the natural frequencies are significantly reduced to 6.7 Hz for Row-L and Row-R, and 3.0 Hz for Row-C due to the fluid added mass effects. For these two cases, the vibration modes show a typical beam vibration and there are no coupled modes between the ducts as shown in Fig. 12. However, for the in-water condition with the fluid coupling mass terms, i.e. CFAM, the 1st natural frequency is almost the same as the previous two cases but the vibration mode shapes are so different and coupled as shown in Fig. 13. In the 1st mode with 2.9 Hz, the vibration of the center duct Row-C is dominant due to a weaker stiffness of the nosepiece than that of Row-L and Row-R. The 2nd mode shape (6.3 Hz) appears as an out-of-phase vibration for Row-L and Row-R due to the coupled fluid effects. As explained in chapter 2.1, this coupled out-of-phase vibration in a water condition coincides well with the case of the submerged concentric cylinders as previously explained in this paper. The 3rd mode is 9.3 Hz and reveals the coupled in-phase vibration of all the ducts.

From the results of the vibration modal analysis, it was shown that the coupled fluid added mass can significantly reduce the core natural frequencies and induce the out-of-phase vibration modes.

3.4 Core seismic behavior

To investigate the fluid effects on the LMR core seismic behavior, the nonlinear seismic time history analyses are carried out for the three conditions used in vibration modal analysis.

The used input seismic motion is the 0.15 g artificial time history with enough numbers of the maximum peaks corresponding to the US NRC Regulatory 1.60 as shown in Fig. 14(a). The time interval of the input motion is 2.0 ms and the total analysis time is 21 seconds. The 3% proportional damping is used for the structure of the ducts. Fig. 14(b) shows the acceleration floor response spectrum for the input motion. As shown in the figure, the frequency components for a strong motion of the input seismic load typically lie between 2.0 Hz and 10.0 Hz.

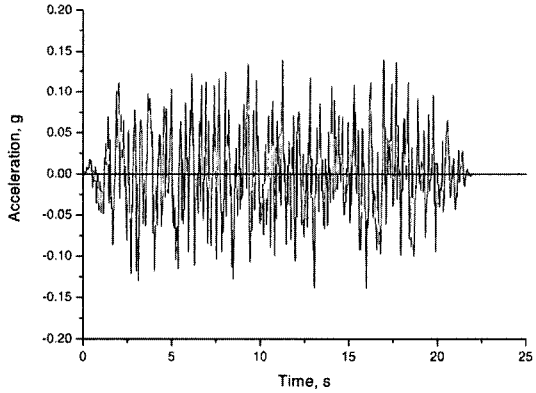

(a) Artificial time history

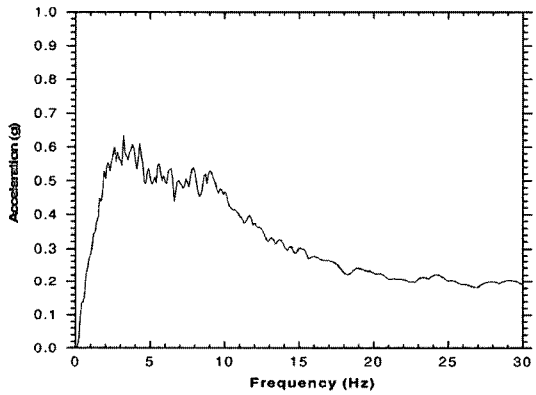

(b) Floor response spectrum of the input motion

Fig. 14 Input seismic motion used in the analysis (US NRC Reg. 1.60)

Figures 15~17 show the analysis results of the displacement time history responses at each top node for the cases of the in-air, in-water without the fluid coupling terms, and the in-water with the fluid coupling terms respectively. As shown in the figures, the maximum displacement seismic responses for the in-air condition are much smaller than the cases of the in-water conditions. From the fact that the natural frequencies in the LMR core will be significantly reduced due to the fluid added mass, it may be deduced that the displacement responses in the cases of the in-water conditions are greatly increased and the impact responses at the gaps are also extensively increased, thus affecting the displacement-impact interaction behavior. From the analysis results, it was revealed that the in-water condition without the fluid coupling terms gives very conservative

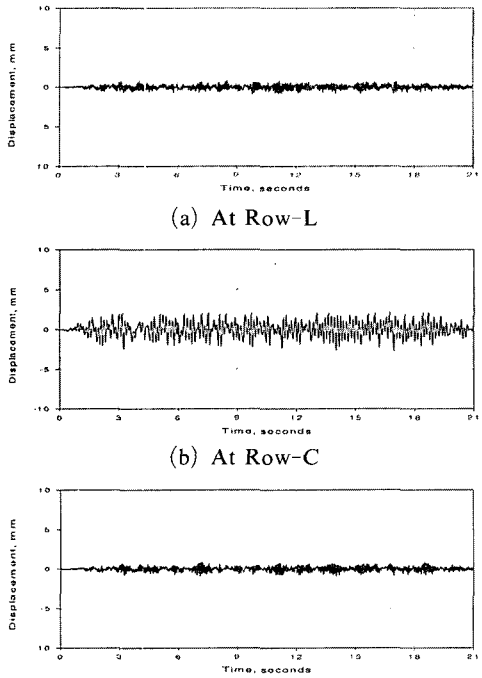

(a) At Row-L

(b) At Row-C

(c) At Row-R

Fig. 15 Displacement responses at the top nodes in air

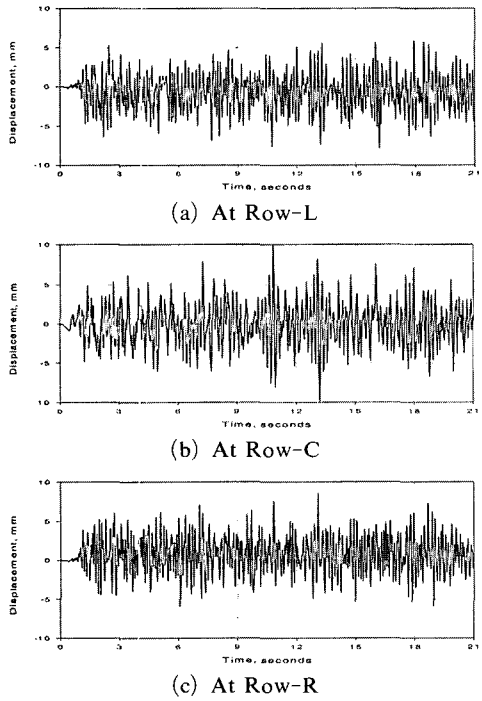

(a) At Row-L

(b) At Row-C

(c) At Row-R

Fig. 16 Displacement responses at the top nodes in water without the fluid coupling terms

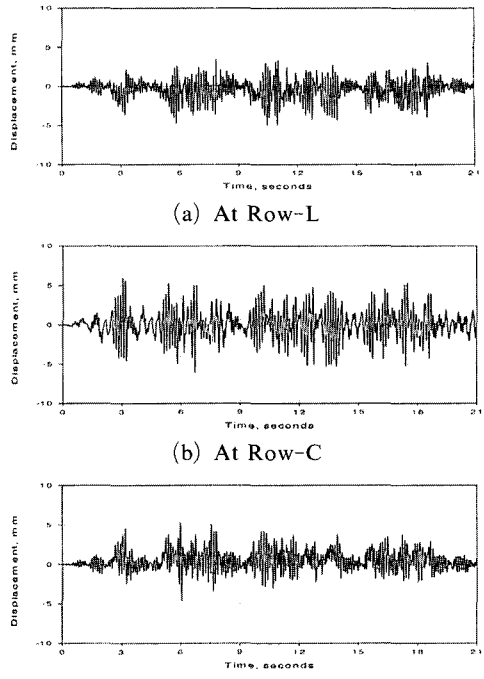

(a) At Row-L

(b) At Row-C

(c) At Row-R

Fig. 17 Displacement Responses at the top nodes in water with the fluid coupling terms

displacement results, much care is required in performing the LMR core seismic analysis with the conventional method when treating the fluid effects by only the diagonal fluid added mass terms.

Figures 18 and 19 show the impact responses at Gap-2 and Gap-3 for each analysis condition respectively. As shown in the figures, the impact responses are very different at each condition. No consideration of the fluid coupling terms gives a severe impact response due to the relatively large displacement responses between the center duct and the outer ducts. This indicates the important role of the fluid coupling terms in the CFAM matrix for the core seismic analysis.

Figure 20 shows the spectrum analysis results by the FFT for the top node of Row-C after the low pass filtering process with a 50 Hz cut-off frequency. In the case of the in-air condition, the dominant peak response appears at 6.4 Hz which exactly corresponds to the 1st natural frequency obtained by the modal analysis. However, for the case of the in-water condition with the CFAM

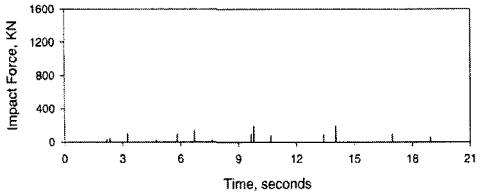

(a) in-Air

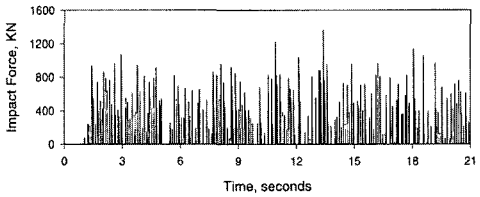

(b) in-Water without fluid coupling terms

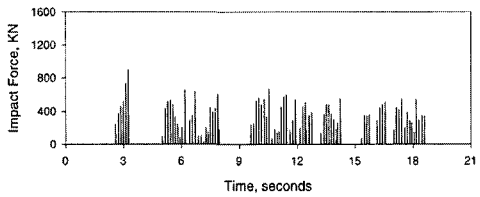

(c) in-Water with fluid coupling terms

Fig. 18 Impact response at gap-2

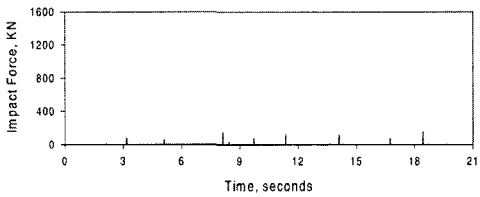

(a) in-Air

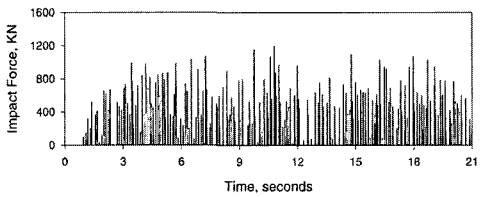

(b) in-Water without fluid coupling terms

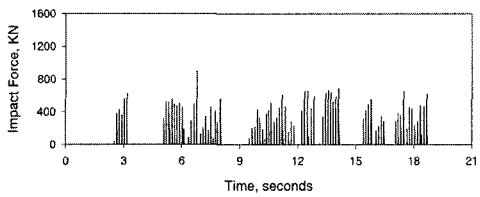

(c) in-Water with fluid coupling terms

Fig. 19 Impact response at gap-3

matrix, the dominant peak response occurs at

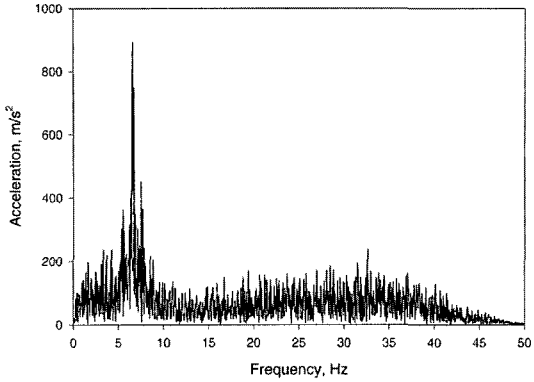

Fig. 20 Frequency response spectrum for Row-C in Air

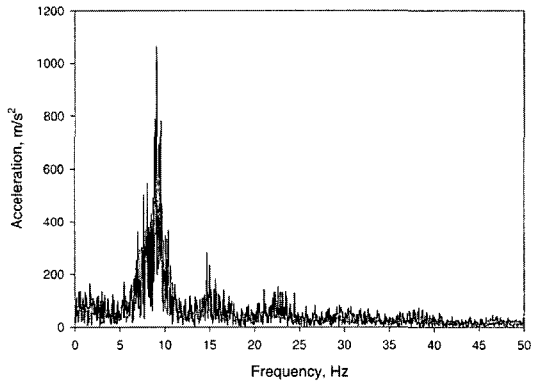

Fig. 21 Frequency response spectrum for Row-C in Water

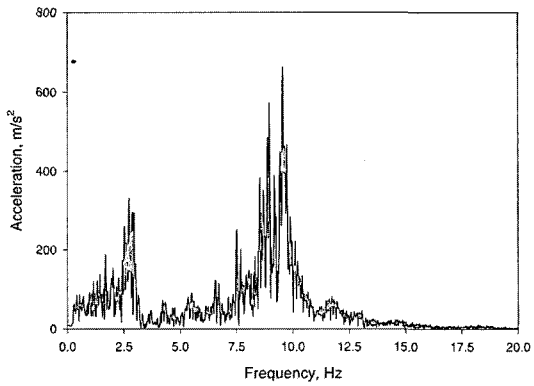

Fig. 22 Frequency response spectrum for Row-C in water with the assumption of no impacts at the gaps

9.3 Hz which corresponds to the 2nd natural frequency, there is no peak response at the 1st natural frequency, 2.9 Hz. The reason is identified

as the severe impact behavior between the center duct and the outer ducts, which invokes a long contact time and suppresses the out-of-phase motion, which is the 1st vibration mode, of the system. To identify these core response characteristics in water, we carried out the analysis for the special condition with the assumption of a very large gap size between the ducts therefore, there was no impact behavior. Figure 21 is the spectrum analysis results. As shown in the figure, we can see that the peak responses clearly appear at 2.9 Hz for the 1st mode and 9.3 Hz for the 2nd mode. This means that the core impact behavior in the water condition with very small gaps between the ducts, which is similar to an actual LMR core system, can severely affect the seismic responses.

4. Conclusions

In this paper, the fluid effects on the LMR core seismic behavior are investigated using the newly developed algorithm by applying the CFAM matrix obtained by the FAMD code to the time history core seismic analysis. From the analysis results for the 7-ducts system with three cases such as the in-air condition and the in-water conditions with and without the fluid coupling terms, it is verified that the dynamic characteristics in the water condition with the fluid coupled added mass terms are very different from the cases of the in-air condition and the in-water condition without the fluid coupled terms. The vibration modes of an immersed LMR hexagonal core duct system have complicated coupled out-of-phase motions due to the coupling terms in the CFAM matrix. These coupled dynamic characteristics can significantly affect the core seismic impact and displacement responses in the LMR core system.

Acknowledgment

This work has been carried out under the Nuclear R&D Program by MOST in Korea.

References

Cook, R. D., Malkus, D. S. and Plesha, M. E., 1989, Concepts and Applications of Finite Element Analysis, Third Edition, John Wiley & Sons.

Fritz, R. J., 1972, "The Effect of Liquids on the Dynamic Motions of Immersed Solids," *Journal of Engineering for Industry, Transactions of the ASME*, pp. 167~173.

Intercomparison of Liquid Metal Reactor Seismic Analysis Codes, 1993, Volume 1 : Validation of Seismic Analysis Codes Using Reactor Core Experiments, IAEA-TECDOC-798.

Intercomparison of Liquid Metal Reactor Seismic Analysis Codes, 1994, Volume 2 : Verification and Improvement of Reactor Code Seismic Analysis Codes Using Core Mock-up Experiments, IAEA-TECDOC-829.

Intercomparison of Liquid Metal Reactor Seismic Analysis Codes, 1995, Volume 3 : Comparison of Observed Effects with Computer Simulated Effects on Reactor Codes from Seismic Disturbances, IAEA-TECDOC-882.

Koo, G. H. and Lee, J. H., 2001, "Effect of Fluid Added Mass on Vibration Characteristics and Seismic Responses of Immersed Concentric Cylinders," *Journal of the Earthquake Engineering Society of Korea*, Vol. 5, No. 5, pp. 25~33.

Koo, G. H. and Lee, J. H., 2003, "Development of FAMD Code to Calculate the Fluid Added Mass and Damping of Arbitrary Structures Submerged in Confined Viscous Fluid," *KSME International Journal*, Vol. 17, No. 3, pp. 457~466.

Koo, G. H. and Lee, J. H., 2003, "Finite Element Analysis for Evaluation of Viscous and Eccentricity Effects on Fluid Added Mass and Damping," *Journal of the Earthquake Engineering Society of Korea*, Vol. 7, No. 2, pp. 21~27.